Eur. Phys. J. B **15**, 87–96 (2000)

THE EUROPEAN PHYSICAL JOURNAL B

EDP Sciences

Distribution of eigenfrequencies for vibrating plates

P. Bertelsen[1], C. Ellegaard[1], and E. Hugues[2,a]

[1] Center for Chaos and Turbulence Studies, Niels Bohr Institute, 2100 Copenhagen Ø, Denmark
[2] Division de Physique Théorique[b], Institut de Physique Nucléaire, 91406 Orsay Cedex, France

Received 5 January 1999 and Received in final form 5 September 1999

Abstract. Acoustic spectra of free plates with a chaotic billiard shape have been measured, and all resonance frequencies in the range 0–500 kHz have been identified. The spectral fluctuations are analyzed and compared to predictions of the Gaussian Orthogonal Ensemble (GOE) of random matrices. The best agreement is found with a superposition of two independent GOE spectra with equal density which indicates that two types of eigenmodes contribute to the same extent. To explain and predict these results a detailed theoretical analysis is carried out below the first cut-off frequency where only flexural and in-plane vibrations are possible. Using three-dimensional plate dispersion relations and two-dimensional models for flexural and in-plane vibrations we obtained two first terms of the asymptotic expansion of the counting function of these eigenmodes. The contribution of edge modes is also discussed. The results are in a very good agreement with the experimentally measured number of modes. The analysis shows that the two types of modes have almost equal level density in the measured frequency interval, and this explains the observed spectral statistics.
For a plate with broken symmetry in the up-down direction (where flexural and in-plane modes are strongly coupled) experimentally observed spectral fluctuations correspond to a single GOE spectrum. Above the first cut-off frequency a greater complexity of the spectral fluctuations is expected since a larger number of types of modes will contribute to the spectrum.

PACS. 03.65.Ge Solutions of wave equations: bound states – 43.40.+s Structural acoustics and vibration – 03.65.Sq Semiclassical theories and applications – 05.45.Mt Semiclassical chaos ("quantum chaos")

1 Introduction

The recent field of physics named quantum chaos [1] has its origin in studies of spectral statistics and semiclassical approximation of quantum systems whose corresponding classical dynamics exhibit chaos. But the ideas and methods of quantum chaos are quite general and can be applied to many other wave phenomena as well, for example they were successfully used in the description of high-frequency resonances in microwave cavities [2,3].

Almost a century ago Weyl [4] started the investigation of high-frequency vibrations of elastic bodies (for related works, see *e.g.* [5]). Recently there has been a renewed interest in the elastodynamical domain because of the link with quantum chaos. In references [8–14] connections between the statistical properties of experimental spectra of vibrations of three-dimensional blocks and Random Matrix Theory (RMT) [6,7] have been discussed, and in reference [15] relations between RMT and the amplitude distribution of acoustic wave functions for plates were investigated. An extension of semiclassical approximation for three-dimensional blocks and for plates was undertaken in references [16–18] and references [19,20] respectively, showing the relevance of the Periodic Orbit Theory for elastodynamics.

In reference [21] it was conjectured that for chaotic quantum systems the statistical properties of spectra are universal on the scale of the mean level spacing. In particular, the spectral fluctuations for models with time reversal invariance and without any space symmetry should be similar to those of random matrices taken from the Gaussian Orthogonal Ensemble (GOE) [6,7]. This universality has been confirmed in a large number of studies, *e.g.* numerically in quantum mechanical models and experimentally using microwave cavities.

In elastodynamics the equations of motion are vectorial, leading, under a certain hypothesis, to longitudinal and transverse wave motions characterized by different sound velocities. Furthermore, depending on the boundary conditions imposed, different waves generally couple at the surface of the body. These characteristics make vibrating solids more difficult to investigate than standard quantum billiards or microwave cavities.

In this paper we consider vibrations of plates below the first cut-off frequency [3] where only a few types of

[a] e-mail: hugues@ipno.in2p3.fr
[b] Unité de Recherche des Universités Paris XI et Paris VI, associée au CNRS

wave motion exist. To describe the motion of the plate we shall use simplified two-dimensional models valid at low frequencies. In [20] flexural vibrations of plates were already studied from a semiclassical point of view. It was numerically shown that spectral fluctuations of flexural modes for a plate with the shape of a chaotic billiard follow the GOE behaviour.

Here we first present the results of experimental measurements of about a thousand eigenfrequencies for chaotic plates. It is demonstrated that experimental spectral fluctuations follow the superposition of two independent GOE-like spectra rather than those of a single GOE spectrum. The main purpose of the paper is to explain this behaviour theoretically. Though it was known in [3] that below the first cut-off frequency there exists only two types of vibrational modes, namely the transversal and in-plane modes, it was assumed that at low frequencies the transversal modes dominate the spectrum. By deriving the Weyl-type formulas [4,5] for the mean number of eigenfrequencies we demonstrate that in the experimental range of frequencies both types of wave motion have approximately the same density. Since these two types of modes are uncoupled for an ideal plate, the resulting spectrum should consist of a superposition of two independent GOE spectra, and this is exactly what we observe experimentally. To check that this phenomenon is connected with the existence of two independent modes, we broke the symmetry of plates in the vertical direction by making small cuts on one side of the plate. This introduces a strong coupling between the flexural and in-plane modes, and we expect to observe spectral fluctuations corresponding to a single GOE spectrum. This was confirmed experimentally.

The plan of the paper is the following. In Section 2 we describe the experimental setup and the results of our experiments. In Section 3 we recall some general properties of three-dimensional elastodynamics. In Section 4 we introduce appropriate two-dimensional models for flexural and in-plane modes, and compute the mean number of eigenfrequencies for both modes with quite a good precision. Finally in the last section, we interpret the experimental data in light of the preceding theoretical analysis. In Appendix A the Rayleigh-Lamb dispersion relations are discussed and in Appendix B we obtain the Weyl expansion for the Poisson model.

2 Experiments

The experimental results presented in this paper are obtained with plates of a special shape called a Sinai stadium. A Sinai stadium is a stadium from which a circle of diameter equal to the length of the straight part has been removed at its center (see Fig. 1). In order to have no geometrical symmetries left, only a quarter of this Sinai stadium was used. Although this system is not completely ergodic it is a convenient model of chaotic motion. This geometry was first used in the context of microwave cavities in reference [22].

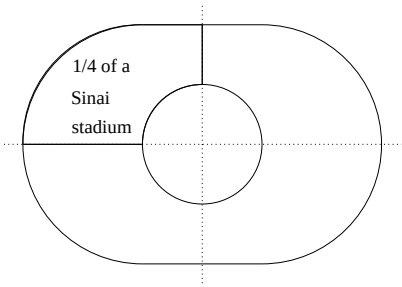

Fig. 1. A quarter of the Sinai stadium shape: from the stadium, a disk whose diameter is equal to the length of the straight wall has been removed from the center.

In our experiments we used Sinai stadium plates made from aluminum with a large radius of 55 mm and a small radius of 29 mm, while the thickness varied from 1 to 10 mm. The experimental apparatus is the same as the one used to study the vibrations of quartz blocks [12–14] (see [12] for a detailed description). To ensure a minimal coupling the plate is excited at a given frequency by a piezoelectric transducer *via* a sapphire stylus (point contact). The response is measured by a similar transducer. The plate is supported by these two styli plus a third passive one. In order to minimize the coupling to the air all experiments were done in vacuum (below 10^{-2} torr). It can thus be assumed that the plate vibrates with free boundary conditions. The quality factor, defined as $Q = f/\Delta f$, where f is the frequency and Δf is the width of a given resonance, was $Q \approx 10\,000$ for the measured spectra. All eigenfrequencies below 500 kHz were identified, providing about a thousand resonances for each plate.

Aluminum was chosen because of its isotropy, its sharp resonances, and because any geometrical shape can be easily produced. The tabulated values of the elastic properties of pure aluminum [23] are $E = 70.3$ GPa for the Young's elastic modulus and $\nu = 0.345$ for the Poisson coefficient. However, these manufactured plates (from [24]) were not made of high-purity aluminum, but only 99.5% pure Al. Needing a great precision in the determination of the Weyl formula, these elastic constants were indirectly measured using the following procedure. For a circular plate the two-dimensional models (see Sect. 4) can be solved exactly, so one can fit the elastic constants such that the calculated eigenfrequencies match with the experimental ones. Considering the first 100 eigenfrequencies, the best agreement found is for $E = 70 \pm 1$ GPa and $\nu = 0.33 \pm 0.005$ [25]. The measured density is $\rho = 2700$ kg/m^3.

To extract the spectral fluctuations the spectrum was unfolded (*i.e.* the eigenfrequencies were divided by the mean level spacing) using the same method as in references [12–14]. However, in order to determine the mean level spacing, a fit based on the analytical Weyl formula (obtained in Sects. 3 and 4) was used instead of a polynomial fit. Then, from the unfolded spectrum, the Nearest Neighbour Spacing Distribution (NNSD) and the Spectral Rigidity ($\Delta_3(L)$) were obtained.

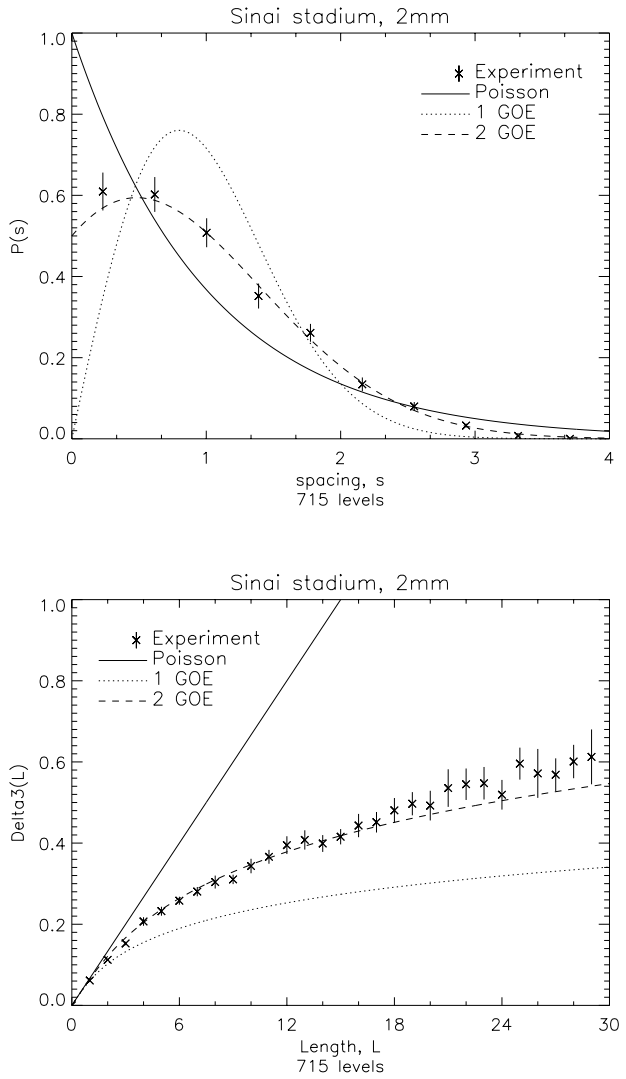

Fig. 2. NNSD (top) and Δ_3 statistics for the measured spectrum of the 2 mm thick quarter of a Sinai stadium plate. Comparison to the Poisson distribution, the single-GOE distribution and the double-GOE distribution with the same weight.

The spectral fluctuations for an integrable shape usually correspond to a Poisson distribution, while those for a chaotic shape usually correspond to a GOE distribution. We have found that for the Sinai stadium plate (see Fig. 2) the spectral fluctuations seem to correspond to a superposition of two independent GOE spectra of equal density. We have excluded the lowest eigenfrequencies in order to improve the statistics, since for a long wavelength, a mode does not "see" the precise geometry of the plate. This result is different from quantum billiards and microwave cavities where an agreement with a single GOE spectrum is found. To explain and predict this result we shall consider in the following sections the plate vibrations from a theoretical point of view.

3 Elastic waves in plates

3.1 Three-dimensional medium

Throughout the paper we shall make the hypothesis of linear elasticity and we shall restrict ourselves to a homogeneous and isotropic material. At any given frequency and for any given direction three waves can propagate independently inside the medium [26,29]. One is a longitudinal wave, called P wave (for "primary" or "pressure"), and the other two are transverse waves, called S waves (for "secondary" or "shear"). Their velocities are given by

$$c_{\mathrm{P}} = \sqrt{\frac{E(1-\nu)}{\rho(1+\nu)(1-2\nu)}}, \quad c_{\mathrm{S}} = \sqrt{\frac{E}{2\rho(1+\nu)}}.$$

These waves generally couple at the surface of the body. In the case of a flat surface, the P wave and the so-called SV wave (V is for vertical), whose displacements are in the incident plane, couple to each other. The so-called SH wave (H is for horizontal), whose displacement is normal to this plane, stay uncoupled (and reflects only into itself). This coupling, which also depends on the angle of incidence, is responsible for the very few exact solutions known in elastodynamics.

3.2 Infinite plates

In the case of an infinite plate, a body limited by two parallel planes, the geometry is so simple that explicit dispersion relations can be obtained [28,29]. Elementary solutions are given by a superposition of incident and reflected waves, whose resulting wave propagates along the plate's plane direction. These propagating waves are of two types:

1. Waves whose displacement is in the incident plane, made of a superposition of P and SV waves: they are called Rayleigh-Lamb (RL) waves.
2. Waves whose displacement is normal to the incident plane, made of a superposition of SH waves.

In the following we shall work with the dimensionless frequency $\Omega = 2\pi f h/c_{\mathrm{S}}$ and the dimensionless wavenumber $K = kh$ where f is the frequency, k is the wave number along the plate's plane direction and h is the thickness of the plate.

For RL waves, the dispersion relation is

$$\frac{\tan(\frac{1}{2}\sqrt{\Omega^2-K^2})}{\tan(\frac{1}{2}\sqrt{\frac{1}{\kappa^2}\Omega^2-K^2})} + \left\{ \frac{4K^2\sqrt{(\Omega^2-K^2)(\frac{1}{\kappa^2}\Omega^2-K^2)}}{(2K^2-\Omega^2)^2} \right\}^{\varepsilon} = 0, \quad (1)$$

where $\kappa = c_{\mathrm{P}}/c_{\mathrm{S}}$ and $\varepsilon = \pm 1$. This relatively simple looking dispersion relation, discovered about a century ago,

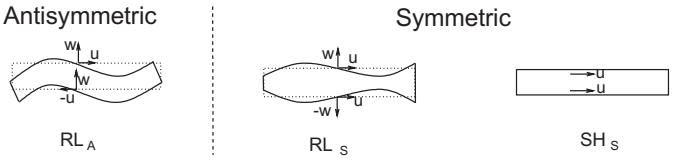

Fig. 3. Illustration of the three wave types for infinite plates and for $\Omega < \pi$: the antisymmetric RL_A wave and the symmetric RL_S and SH_S waves. The symmetry properties of the displacement components (u, w) relative to the middle plane of the plate is also shown in this exaggerated figure: for an antisymmetric wave, u is odd and w is even, and for a symmetric wave, u is even and w is odd.

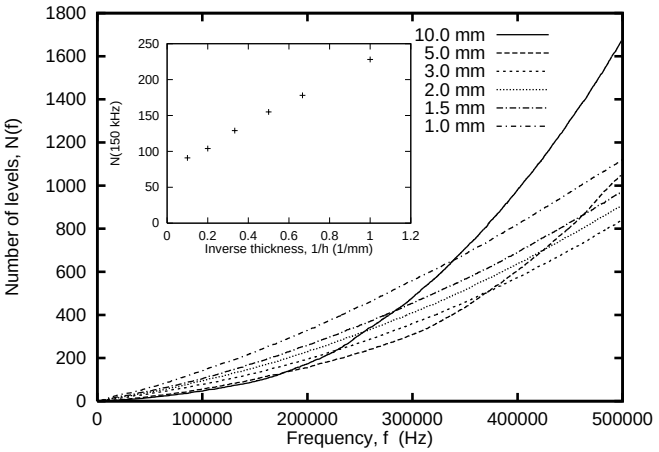

Fig. 4. Experimental staircase function for the Sinai stadium plates of thicknesses varying between 1 and 10 mm. Insert: value of the staircase function at 150 kHz as a function of the inverse thickness.

has an intricate behaviour, which was not completely understood until only forty years ago [30]. Due to the mirror symmetry of the plate with respect to its middle plane, two types of waves are possible. The first is called symmetric, since the components of the displacements parallel and normal to this middle plane are respectively even and odd with respect to the symmetry (see Fig. 3). The second type is called antisymmetric, since these components are respectively odd and even. Symmetric waves are called *in-plane* waves since their mean displacement along a line normal to the middle plane is along this plane. Correspondingly, antisymmetric waves are called *flexural* waves since their mean displacement is normal to the middle plane. In equation (1) $\varepsilon = +1$ describes symmetric waves and $\varepsilon = -1$ describes antisymmetric waves. At a given frequency only a finite number of propagating waves exist, each belonging to a different family. Each family is bounded from below by a certain cut-off frequency. Below the first one, *i.e.* for $\Omega < \pi$, only two families coexist; one symmetric (denoted hereafter RL_S) and one antisymmetric (denoted RL_A).

For SH waves, the dispersion relation is

$$\Omega^2 = K^2 + (n\pi)^2, \tag{2}$$

for the nth family of waves, where n is a positive integer. Here we clearly see that the nth family only exists above the cut-off frequency $n\pi$. When $\Omega < \pi$, only the family $n = 0$ exists, which is symmetric and is denoted SH_S (see Fig. 3).

Above the first cut-off frequency $f_c = \frac{c_S}{2h}$ the wavelength is sufficiently small to permit the presence of a nodal point in the thickness direction. So intuitively, f_c is the frequency above which these waves become three-dimensional waves. The effect of these cut-off frequencies can clearly be seen for finite plates on the eigenfrequencies counting function (staircase function) as shown in Figure 4 where the measured spectra of plates with thicknesses from 1 mm to 10 mm are plotted. Since the measured frequency interval is 0–500 kHz, the effect is only visible for $h = 5$ mm where $f_c = 312.2$ kHz, and for $h = 10$ mm where $f_c = 156.1$ kHz. Above any cut-off frequency a new wave family appears, causing a sudden increase in the slope of the staircase function.

3.3 Finite plates

We now consider plates bounded by edges, which do not break the symmetry of the plate relative to its middle plane. To satisfy the free edge boundary conditions, a superposition of the propagating RL and SH waves occurs for each eigenfrequency. But besides these waves there exist, due to the finiteness of the plate, a number of edge waves corresponding to solutions of (1) and (2) with complex values of K [28,29]. The edge waves are characterized by the condition that the mean displacement decreases exponentially as a function of the distance from the edge. The presence of these edge waves makes the calculation of the scattering phase of the propagating waves difficult.

To extract the approximate scattering phase, one can use a high order two-dimensional model (derived from the three-dimensional equations) which approximately takes these edge waves into account in the frequency range of interest [31]. Furthermore, in the symmetric case equation (1) has a complex branch of solutions beginning at zero frequency, and it was shown both theoretically [31] and experimentally [32] that this branch contributes to the edge waves. A study of a high order two-dimensional model has shown that for $\Omega < \pi$ the Poisson model (described in Sect. 4.2) is sufficient to estimate the Weyl formula. The effect of the edge waves will be further discussed in Section 5.

Since the boundary conditions at the edge do not break the symmetry, there are symmetric eigenmodes (made

mainly of SH_S and RL_S waves) and antisymmetric eigenmodes (made mainly of RL_A waves). These two types of eigenmodes explain why the observed spectral fluctuations seem to be those of a superposition of two independent spectra (Fig. 2).

In the following we shall estimate the Weyl formula using the asymptotic expansion of the staircase function $N(f) = \sum_n \Theta(f - f_n)$ at large f. The first main term (the surface term) is

$$N(f) \sim \frac{S}{4\pi h^2} \sum_m K_m^2(\Omega), \tag{3}$$

where S is the surface area of the plate and $K_m(\Omega)$ is the value of K for the wave family m at the frequency Ω, given by the corresponding dispersion relation.

In the region of interest (*i.e.* $\Omega < \pi$) the RL_S and RL_A dispersion relations obtained from (1) can be approximated by:

$$K_{RL_S}(\Omega) \approx \frac{1}{\kappa'}\Omega[1 + a_{S,1}\Omega^2 + a_{S,2}\Omega^4 + b_S\Omega^6], \tag{4}$$

$$K_{RL_A}(\Omega) \approx \frac{12^{1/4}}{\sqrt{\kappa'}}\sqrt{\Omega}[1 + a_{A,1}\Omega + a_{A,2}\Omega^2 + b_A\Omega^3], \tag{5}$$

where $\kappa' = \sqrt{2/(1-\nu)}$. The a's are the true coefficients of the expansions, and the b's are fitted such that these expressions lead to errors less than one level for the mean staircase function (see Appendix A). For SH_S waves the dispersion relation (2) gives:

$$K_{SH_S}(\Omega) = \Omega. \tag{6}$$

However, in order to describe precisely what is happening in the experiments we have to know the staircase function accurately, and considering only the surface term in its asymptotic expansion is clearly not sufficient. In the following section we introduce two-dimensional models of plates for which the following asymptotic term, proportional to the perimeter, can be evaluated. The perimeter term takes into account the boundary conditions and the scattering phase of the waves. The precision needed will then be attained using not the dispersion relations of these two-dimensional models but the three-dimensional ones (see Eqs. (4, 5, 6))

4 Two-dimensional plate models

At this stage, we can relate the three-dimensional analysis to the approximate two-dimensional models describing the motion of the middle plane of the plate (see [26–29]). We have chosen the simplest models describing what is happening below the first cut-off frequency.

4.1 A model for the flexural waves

Assuming that a line normal to the middle plane remains straight after the deformation and normal to the deflected surface, the following biharmonic equation for the transverse displacement w of the middle plane is found:

$$\rho h \frac{\partial^2 w}{\partial t^2} = -D\Delta^2 w, \tag{7}$$

where $D = \frac{Eh^3}{12(1-\nu^2)}$ is the flexural rigidity and Δ is the two-dimensional Laplacian operator. This flexural model is called the Kirchhoff-Love model [26,29]. In a curvilinear coordinate system (l, n), where at the edge, l is the curvilinear abscissa and n is the normal coordinate positive at the interior of the domain, the free edge boundary conditions are

$$\frac{\partial^3 w}{\partial n^3} + (2-\nu)\left(\frac{\partial^3 w}{\partial l^2 \partial n} + \frac{\mathrm{d}C}{\mathrm{d}l}\frac{\partial w}{\partial l}\right) + 3C\frac{\partial^2 w}{\partial l^2} - (1+\nu)C^2\frac{\partial w}{\partial n} = 0$$
$$\frac{\partial^2 w}{\partial n^2} + \nu\frac{\partial^2 w}{\partial l^2} - \nu C\frac{\partial w}{\partial n} = 0 \tag{8}$$

where $C(l)$ is the curvature of the edge, and $\partial/\partial l$ and $\partial/\partial n$ respectively denote the tangent and normal derivatives at the edge. The dispersion relation is ($\mathcal{K}$ denoting "Kirchhoff-Love")

$$K_{\mathcal{K}} = \frac{12^{1/4}}{\sqrt{\kappa'}}\sqrt{\Omega},$$

which is exactly the first term of (5). This proves that this model represents the RL_A waves at small frequency, *i.e.* when $K_{\mathcal{K}} \ll 1$. It was studied semiclassically in [20], and the asymptotic expansion of the staircase function reads

$$N_{\mathcal{K}}(K_{\mathcal{K}}) = \frac{S}{4\pi h^2}K_{\mathcal{K}}^2 + \beta_{\mathcal{K}}(\nu)\frac{L}{4\pi h}K_{\mathcal{K}} + o(K_{\mathcal{K}}), \tag{9}$$

for a plate of surface area S and perimeter L. $\beta_{\mathcal{K}}(\nu)$ is given by

$$\beta_{\mathcal{K}}(\nu) = -1 + 4\left[\nu'(2-3\nu') + 2\nu'\sqrt{2\nu'^2 - 2\nu' + 1}\right]^{-1/4}$$
$$-\frac{4}{\pi}\int_0^1 \arctan\left[\frac{\sqrt{1-t^2}}{\sqrt{1+t^2}}\left(\frac{1+\nu' t^2}{1-\nu' t^2}\right)^2\right]\mathrm{d}t, \tag{10}$$

where $\nu' = (1-\nu)$. For aluminum, $\beta_{\mathcal{K}}(0.33) = 1.7125908$. It was shown in [20] that the spectral fluctuations follow the GOE behavior for a chaotic shape.

4.2 A model for the in-plane waves

Assuming the plane stress hypothesis, *i.e.* that transverse stresses which vanish at the free surfaces also vanish inside

the plate, one finds the following vectorial equation for the in-plane displacement $\mathbf{u}$ of the middle plane:

$$\frac{\partial^2 \mathbf{u}}{\partial t^2} = {c_{\mathrm{P}'}}^2 \boldsymbol{\nabla}(\boldsymbol{\nabla}\cdot\mathbf{u}) - {c_{\mathrm{S}}}^2 \boldsymbol{\nabla}\times\boldsymbol{\nabla}\times\mathbf{u}, \qquad (11)$$

where $c_{\mathrm{P}'} = \kappa' c_{\mathrm{S}}$ and where the differential operators are two-dimensional. The approximate model for in-plane wave motion is known as the Poisson model [28]. The free edge boundary conditions are simply obtained by writing that the stresses vanish at the edge.

Except that the constants differ, the equations of motion for this model have exactly the same form as those for plane strain. Therefore, the same kind of wave motion takes place. A transverse S wave with velocity c_{S} coexists with a longitudinal P′ wave with velocity $c_{\mathrm{P}'}$ smaller than c_{P}. The dispersion relation of the P′ waves is the first term of (4) so they represent the $\mathrm{RL_S}$ waves at small frequency, *i.e.* for $K_{\mathcal{P}} \ll 1$ ($\mathcal{P}$ denoting "Poisson"). The dispersion relation of the S waves is exactly (6), which shows that they represent the $\mathrm{SH_S}$ waves. As in three dimensions the P′ and S waves couple at the edge of the plate. Semiclassically, this gives rise to ray splitting, which enhances the chaoticity of the ray trajectories [16,17].

Vasil'ev [33] has given the second term of the asymptotic expansion of the staircase function which reads

$$N_{\mathcal{P}}(K_{\mathcal{P}}) = \frac{S}{4\pi h^2}\left(1+\frac{1}{{\kappa'}^2}\right)K_{\mathcal{P}}^2 + \beta_{\mathcal{P}}(\nu)\frac{L}{4\pi h}K_{\mathcal{P}} + o(K_{\mathcal{P}}). \qquad (12)$$

To our knowledge $\beta_{\mathcal{P}}(\nu)$ was first calculated in [34] but with some errors. Its correct expression (see Appendix B) is

$$\beta_{\mathcal{P}}(\nu) = \frac{4}{\sqrt{s_0(\nu)}} - 3 + \frac{1}{\kappa'} + \frac{4}{\pi}\int_{1/\kappa'}^{1} \arctan\left[\frac{(2t^2-1)^2}{4t^2\sqrt{1-t^2}\sqrt{t^2-\frac{1}{{\kappa'}^2}}}\right]\mathrm{d}t. \qquad (13)$$

For aluminum $\beta_{\mathcal{P}}(0.33) = 2.0857543$.

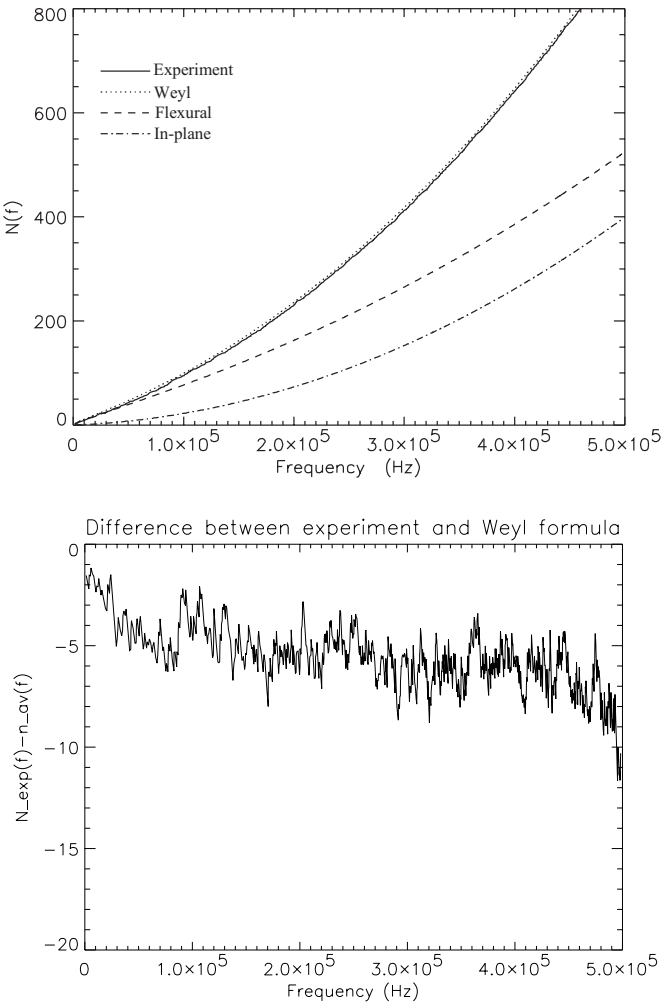

Fig. 5. Above: comparison between the experimental staircase function (solid line) for the 2 mm thick quarter of a Sinai stadium plate and the theoretical mean one (dotted line). The flexural (dashed line) and the extensional (dashed/dotted line) contributions to the latter are also given. Below: difference between the experimental staircase function and the theoretical mean one.

5 Discussion of the results

The number of eigenfrequencies below a given frequency depends on the plate thickness h as shown in Figure 4. As it can be seen from the Weyl formula, this dependency is mostly due to the flexural modes, and is mainly contained in the surface term

$$\frac{\sqrt{3}Sf}{\kappa' c_{\mathrm{S}} h}$$

which varies as $1/h$. This behaviour is clearly seen in the insert of Figure 4, which plots the number of levels below 150 kHz as a function of $1/h$.

Special care is needed for the edge modes, which contribute to the perimeter terms of the mean staircase function. In the flexural case [20], the transverse displacement of such a mode decreases as $\exp(-\alpha_{\mathrm{fl}} k_{\mathcal{K}} y)$ where y is the distance from the edge and $\alpha_{\mathrm{fl}} = \sqrt{1/\kappa_{\mathcal{K}}^2(\nu) - 1} = 0.0548$ (see [20], Eq. (20) for the definition of $\kappa_{\mathcal{K}}(\nu)$), so we regard them as measurable. Similarly, in the in-plane case the displacement of a Rayleigh mode decreases as $\exp(-\alpha_{\mathrm{in}} k_{\mathcal{P}} y)$ where $\alpha_{\mathrm{in}} = \sqrt{1 - s_0(\nu)} = 0.3941$ (see Appendix B for the definition of $s_0(\nu)$). Such a value indicates that these modes will only be detected experimentally if the transducer is close to the edge of the plate. Actually we expect the edge waves to couple to the interior waves, especially at the corners, a mechanism which makes the edge modes

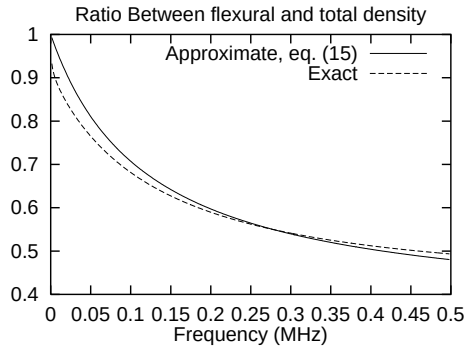

Fig. 6. Ratio of the mean flexural level density to the total mean density for the 2 mm thick quarter of a Sinai stadium aluminum plate as a function of frequency: the approximate ratio (dashed line) and the exact one (solid line) given by equation (15)

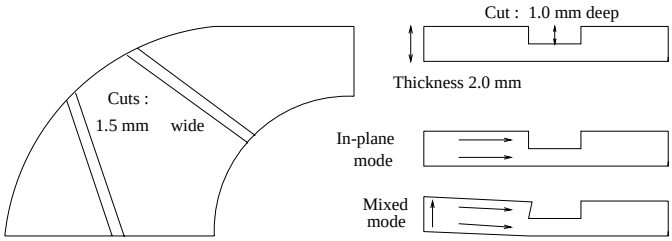

Fig. 7. The 2 mm thick quarter of a Sinai stadium plate with broken symmetry: two 1 mm deep cuts have been made. For example, it is shown how one cut turns an in-plane wave into a "mixed" wave.

easier to detect. Therefore we include them in the Weyl formula.

A very good agreement is found between the experimental staircase function and the theoretical mean one, as shown in Figure 5. Less levels than predicted are found in the experimental spectra. The difference oscillates at small frequencies around 2, then around approximately 6, to attain about 10 at 500 kHz. A similar behaviour was found for other thicknesses and shapes. In the case of a quantum billiard this difference oscillates around a constant value, which is the third term in the asymptotic expansion of the staircase function. As the NNSD statistics (see Fig. 2) shows no level repulsion, this difference can be due to almost degenerate levels identified as one level. Another explanation can be the lack of detection of some Rayleigh modes, whose number is essentially independent of the thickness, and whose contribution to the mean staircase is quasi-linear. Finally, we must recall that the elastic constants are only known within about 1% (see Sect. 2). Such an uncertainty may cause a nonlinear discrepancy, giving potentially a maximum deviation of 5 levels (for each elastic constant). In conclusion, since this agreement is mainly thickness-independent and shape-independent in our experiments, we may infer that it validates both the theoretical and the experimental part of our study.

To predict the spectral fluctuations, one needs to know the relative mean density of flexural and in-plane modes. The mean level density is the slope of the mean staircase function, which to a good approximation is described by the surface term. Then the mean flexural and in-plane staircases can be written

$$\bar{N}_{\mathrm{fl}}(\Omega) \approx \frac{S}{4\pi h^2}\frac{\sqrt{12}}{\kappa'}\Omega[1+2a_{\mathrm{A},1}\Omega],$$

$$\bar{N}_{\mathrm{in}}(\Omega) \approx \frac{S}{4\pi h^2}(1+\frac{1}{\kappa'^2})\Omega^2, \qquad (14)$$

where the next smaller terms in equations (4, 5) have been neglected. From these expressions the relative mean flexural density can be expressed by

$$\frac{\bar{\rho}_{\mathrm{fl}}}{\bar{\rho}} \approx \frac{1+\frac{(17-7\nu)}{10\sqrt{6(1-\nu)}}\Omega}{1+\frac{(47-17\nu)}{10\sqrt{6(1-\nu)}}\Omega}\,. \qquad (15)$$

In this approximation the relative mean densities are shape-independent which is corroborated by the observed spectral fluctuations. The precision of this approximation is shown in Figure 6 where it is compared to the exact value. The in-plane mean density of modes vanishes at low frequency, since it is proportional to the frequency. However, already around the first tens of levels, the in-plane relative mean density is no longer negligible. The relative mean flexural density decreases rapidly to a value close to 1/2. Since the level density increases with frequency, the preceding value will concern the majority of the levels. The spectral fluctuations should then be close to those of a superposition of two independent spectra of almost equal densities. This is effectively what is observed, both for the Sinai Stadium shape (see Fig. 2) and also for other chaotic shapes. For chaotic shapes, each of the two independent spectra follow the GOE behavior, a fact that was expected as mentioned in the previous sections. That we observe two GOE spectra of almost exactly equal level density is also related to the fact that the statistical observables are not very sensitive to small changes in the relative densities around 1/2. For example, a superposition with relative densities of 0.65 and 0.35 would give almost the same result.

To confirm that we effectively observe a superposition of independent spectra due to the symmetry of the plate in the thickness direction, we broke the symmetry by making two cuts (1 mm deep) on one side of the 2 mm thick Sinai stadium plate as shown in Figure 7.

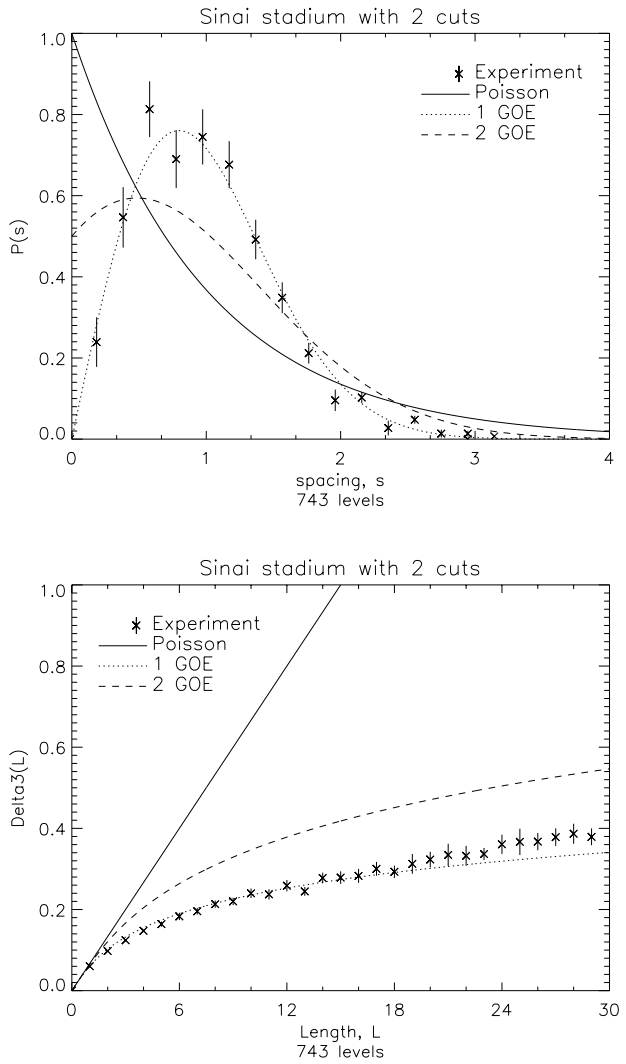

Fig. 8. NNSD (top) and Δ_3 (bottom) statistics for the measured spectrum of the Sinai stadium plate with two cuts. Comparison to the Poisson distribution, the single-GOE distribution and the double-GOE distribution with the same weight.

As expected, the spectral fluctuations shown at Figure 8 clearly follow those of a single GOE spectrum.

It has been mentioned in Section 3 that the in-plane modes were made of $\mathrm{RL_S}$ and $\mathrm{SH_S}$ waves *i.e.* of longitudinal and transverse waves which couple at the edges of the plate. But the question of the existence of purely longitudinal or transverse modes has not been addressed here: this can hardly be seen from the experimental results as the longitudinal waves contribute to the total mean number of modes (see Eq. (3)) to only about 10%. Recently, a closer look at the in-plane modes [35] which have been separated from the flexural ones has demonstrated that comparing the experimental data to a RMT model the longitudinal and transverse modes may not be fully coupled.

6 Conclusions

High frequency spectra of free aluminum plates have been measured. Below the first cut-off frequency both flexural and in-plane modes contribute because of the symmetry of the plate in the thickness direction. Their approximate theoretical mean staircase function is given up to the perimeter term, using two-dimensional models of real plates. The very good agreement between the experimental and the theoretical staircase function validates both parts of the study.

The flexural and the in-plane spectra are shown to have almost equal density at high frequency, a fact which explains why for classically chaotic shapes the spectral fluctuations observed are very close to those of a superposition of two GOE spectra of equal density. This will be the case for all boundary conditions which do not break the symmetry, *i.e.* not only for the present free edge boundary conditions. When the symmetry is broken by cuts made in the plate, the different modes couple completely and a single GOE distribution is observed. Above the first cut-off frequency new families of modes appear which, correspondingly, will increase the complexity of the spectral fluctuations.

The authors are greatly indebted to E. Bogomolny, K. Schaadt, C. Schmit, M. Oxborrow and T. Guhr for numerous fruitful discussions. This work was supported by the Danish National Research Council, and one of the authors (E.H.) was supported by the French Ministry of Education and Research (MENESR).

Appendix A: Rayleigh-Lamb dispersion relations expansion

In order to write the Weyl expansion of the plate's staircase function as powers of Ω we present here the expansions of $K_m(\Omega)$ for the Rayleigh-Lamb modes obtained from the dispersion relation (1). Due to the fact that the function to be approximated has many singularities, the expansion will have bad convergence properties. To obtain a precision of one level in the staircase function for $\Omega < \pi$, the expansion is truncated when it fits best, and the next coefficient is fitted to ensure the required precision.

For the symmetric $\mathrm{RL_S}$ mode, the expansion required is given by (4), where

$$a_{\mathrm{S},1}(\nu) = \frac{\nu^2}{48(1-\nu)},$$

$$a_{\mathrm{S},2}(\nu) = \frac{\nu^2(7\nu^2 - 40\nu + 24)}{23040(1-\nu)^2}, \tag{16}$$

where the last term was obtained using *Mathematica* [36]. For aluminum, $a_{\mathrm{S},1} = 3.386194 \times 10^{-3}$ and $a_{\mathrm{S},2} = 1.217419 \times 10^{-4}$, and the next fitted coefficient is $b_{\mathrm{S}} = 6.5296 \times 10^{-6}$, leading to a maximal error of 5×10^{-4}.

For the antisymmetric $\mathrm{RL_A}$ mode, the expansion [37] retained is given by (5), with

$$a_{\mathrm{A},1}(\nu) = \frac{\sqrt{6}(17-7\nu)}{240\sqrt{1-\nu}},$$
$$a_{\mathrm{A},2}(\nu) = \frac{607\nu^2+1726\nu-1353}{134400(1-\nu)}. \quad (17)$$

The next term of the expansion is an order of magnitude bigger than the preceding one, due to the small radius of convergence of the series. For aluminum, $a_{\mathrm{A},1} = 0.183\,167\,7$ and $a_{\mathrm{A},2} = -7.965\,948\times10^{-3}$, and the next fitted coefficient is $b_{\mathrm{A}} = 8.679\,5\times10^{-4}$, leading to a maximal error of 4×10^{-3}.

Appendix B: Weyl expansion for the Poisson model

In this appendix we derive the two first terms of the asymptotic expansion of the staircase function for the Poisson model. The general method for two-dimensional problems has been exposed in detail in [20], especially in Appendix A.

The dominating term proportional to the surface area is easily obtained from the eigenvalues of the differential operator and the result is

$$\tilde{N}_1(\omega) = \frac{S}{4\pi}\left(1+\frac{1}{\kappa'^2}\right)\left(\frac{\omega}{c_{\mathrm{S}}}\right)^2, \quad (18)$$

where $\omega = 2\pi f$.

Vasil'ev [33] has given the general expression for the next term of the form

$$\tilde{N}_2(\omega) = \beta_{\mathcal{P}}(\nu)\frac{L}{4\pi}\frac{\omega}{c_{\mathrm{S}}}, \quad (19)$$

where L is the perimeter of the plate. As the Poisson and plane strain equations are of the same form, the calculation of this term in [34] can be used here. However, some errors were found, which we correct here.

$\beta_{\mathcal{P}}(\nu)$ is made of two contributions. The first one comes from the discrete spectrum (see [20]) which is represented here by the Rayleigh modes propagating along the edge, and exponentially decaying from it. This contribution is

$$\beta_{\mathrm{d.s.}}(\nu) = \frac{4}{\sqrt{s_0(\nu)}}, \quad (20)$$

where $s_0(\nu)$ is the unique root in the interval $]0,1[$ of the following polynomial

$$s^3 - 8s^2 + 8\left(3-\frac{2}{\kappa'^2}\right)s - 16\left(1-\frac{1}{\kappa'^2}\right) = 0. \quad (21)$$

The other contribution comes from the continuous spectrum. For the 1-dimensional straight-line edge problem the scattering of waves at the edge can be described by the scattering matrix $S(p,\omega)$ for a wave vector component p along the edge. The contribution is made of the total phase of the scattering matrix defined, up to a constant, by

$$\phi(p,\omega) = \arg\det S(p,\omega). \quad (22)$$

But this formula is valid only between the singular points of the spectrum at which the dimension of the S-matrix changes and where the phase is discontinuous. In our case the dimension changes by one and we have a hard singular point corresponding to a Dirichlet boundary condition which gives a phase jump of $-\frac{\pi}{2}$. To define the phase completely its origin is defined in such a way that it will not contribute when the continuous spectrum is absent. Following these rules which were not entirely satisfied in [34] we get from the definition of the continuous spectrum contribution

$$\beta_{\mathrm{c.s.}}(\nu) = \frac{1}{\pi}\int \mathrm{d}p\,\frac{\phi(p,1)}{2\pi}, \quad (23)$$

the following expression:

$$\beta_{\mathrm{c.s.}}(\nu) = -3 + \frac{1}{\kappa'} + \frac{4}{\pi}\int_{1/\kappa'}^{1} \arctan\left[\frac{(2t^2-1)^2}{4t^2\sqrt{1-t^2}\sqrt{t^2-\frac{1}{\kappa'^2}}}\right]\mathrm{d}t. \quad (24)$$

In conclusion, following [33] we can write

$$N_{\mathcal{P}}(\omega) = \frac{S}{4\pi}\left(1+\frac{1}{\kappa'^2}\right)\left(\frac{\omega}{c_{\mathrm{S}}}\right)^2 + \beta_{\mathcal{P}}(\nu)\frac{L}{4\pi}\frac{\omega}{c_{\mathrm{S}}} + o(\omega), \quad (25)$$

where $\beta_{\mathcal{P}} = \beta_{\mathrm{d.s.}} + \beta_{\mathrm{c.s.}}$.

This expression has been validated using the integrable circular plate, for various values of ν.

References

1. *Chaos and Quantum Physics, Proc. of Les Houches Summer School of Theoretical Physics, 1989*, edited by M.-J. Giannoni, A. Voros, J. Zinn-Justin (North Holland, Amsterdam, 1991).
2. R. Balian, B. Duplantier, Ann. Phys. N.Y. **104**, 300 (1977); O. Frank, B. Eckhardt, Phys. Rev. E **53**, 4166 (1996).
3. H.-J. Stöckmann, J. Stein, Phys. Rev. Lett. **64**, 2215 (1990); U. Stoffregen, J. Stein, H.-J. Stockmann, M. Kuś, F. Haake, *ibid.* **74**, 2666 (1995); H.D. Gräf, H.L. Harney, H. Lengeler, C.H. Lewenkopf, C. Rangacharyulu, A. Richter, P. Schardt, H.A. Weidenmüller, *ibid.* **69**, 1296 (1992); H. Alt, H.-D. Gräf, H.L. Harney, R. Hofferbert, H. Lengeler, A. Richter, P. Schardt, H.A. Weidenmüller, *ibid.* **74**, 62 (1995).
4. H. Weyl, Nachr. Akad. Wiss. **110**, Göttingen (1911); H. Weyl, Rend. Circ. Mat. Palermo **39**, 1 (1915); for the solid

sphere, see: P. Debye, Ann. Phys. Leipzig **39**, 789 (1912).
5. H.P. Baltes, E.R. Hilf, *Spectra of finite systems* (Bibliographisches Institut, Mannheim, 1976).
6. M.L. Mehta, *Random Matrices* (Academic Press, 2nd ed., Boston, 1991).
7. T. Guhr, A. Müller-Groeling, H.A. Weidenmüller, Phys. Rep. **299**, 189 (1998).
8. R.L. Weaver, J. Acoust. Soc. Am. **85**, 1005 (1989).
9. O. Bohigas, O. Legrand, C. Schmit, D. Sornette, J. Acoust. Soc. Am. **89**, 1456 (1991).
10. D. Delande, D. Sornette, R. Weaver, J. Acoust. Soc. Am. **96**, 1873 (1994).
11. C. Ellegaard, T. Guhr, K. Lindemann, H.Q. Lorensen, J. Nygård, M. Oxborrow, Phys. Rev. Lett. **75**, 1546 (1995).
12. M. Oxborrow, C. Ellegaard, *Proceedings of the 3rd International Conference on Experimental Chaos*, *Edinburgh 1995* (World Scientific, 1996), pp. 251-260.
13. C. Ellegaard, T. Guhr, K. Lindemann, J. Nygård, M. Oxborrow, *Proceedings of the IVth Wigner Symposium in Guadalajara, Mexico*, edited by N.M. Alakishiyev, T.H. Seligman, K.B. Wolf (World Scientific, Singapore, 1996), pp. 330-333.
14. C. Ellegaard, T. Guhr, K. Lindemann, J. Nygård, M. Oxborrow, Phys. Rev. Lett. **77**, 4918 (1996).
15. K. Schaadt, M.Sc. Thesis, CATS, Niels Bohr Institute (1997), `http://www.nbi.dk/~schaadt/speciale/speciale.ps.gz`.
16. L. Couchman, E. Ott, T.M. Antonsen Jr, Phys. Rev. A **46**, 6193 (1992); L.S. Schuetz, Ph.D. Thesis, University of Maryland (1991).
17. R.E. Prange, E. Ott, T.M. Antonsen Jr., B. Georgeot, R. Blümel, Phys. Rev. E **53**, 207 (1996); R. Blümel, T.M. Antonsen Jr, B. Georgeot, E. Ott, R.E. Prange, Phys. Rev. Lett. **76**, 2476 (1996); R. Blümel, T.M. Antonsen Jr, B. Georgeot, E. Ott, R.E. Prange, Phys. Rev. E **53**, 3284 (1996).
18. N. Søndergaard, M. Sc. Thesis, CATS, Niels Bohr Institute (1996), `http://www.nbi.dk/~nsonderg/speciale/.`
19. O. Legrand, C. Schmit, D. Sornette, Europhys. Lett. **18**, 101 (1992).
20. E. Bogomolny, E. Hugues, Phys. Rev. E **57**, 5404 (1998).
21. O. Bohigas, M.-J. Giannoni, C. Schmit, Phys. Rev. Lett. **52**, 1 (1984); J. Phys. France **45**, L1015 (1984).
22. A. Kudrolli, S. Sridhar, A. Pandey, R. Ramaswamy, Phys. Rev. E **49**, R11 (1994).
23. G.W.C. Kaye, T.H. Laby, *Tables of Physical and Chemical Constants* (Longman, London, 1986).
24. NKT Metalgården A/S, Denmark.
25. P. Bertelsen, M.Sc. Thesis, CATS, Niels Bohr Institute (1997), `http://www.nbi.dk/~pbertel/plates/speciale.ps.gz.`
26. A.E.H. Love, *A Treatise on The Mathematical Theory of Elasticity* (Dover, New York, 1944).
27. L.D. Landau, E.M. Lifshitz, *Theory of Elasticity* (Pergamon Press, London, 1959).
28. J.D. Achenbach, *Wave Propagation in Elastic Solids*, Series in Applied Mathematics and Mechanics, Vol. 16 (North Holland, 2nd ed., Amsterdam, 1976).
29. K.F. Graff, *Wave Motion in Elastic Solids* (Dover, New York, 1991).
30. R.D. Mindlin, in *Structural Mechanics*, edited J.N. Goodier, N.J. Hoff (Pergamon Press, New York, 1960).
31. D.C. Gazis, R.D. Mindlin, J. Appl. Mech. **541** (1960).
32. E.A.G. Shaw, J. Acoust. Soc. Am. **28**, 38 (1956).
33. D.G. Vasil'ev, Trans. Moscow Math. Soc. **49**, 173 (1987).
34. K. Lotfi, Ph.D. Thesis, Université Paris-Sud (1995).
35. A. Andersen, M.Sc. Thesis, Niels Bohr Institute (1999), `http://www.nbi.dk/~aanders/thesis.ps.`
36. S. Wolfram, *Mathematica, a system for doing mathematics by computer* (Addison Wesley, 2nd ed., Redwood City, 1991).
37. F.I. Niordson, Int. J. Solids Struct. **15**, 167 (1979).